Spectrochimica Acta Part A 72 (2009) 663–669

Contents lists available at ScienceDirect

Spectrochimica Acta Part A: Molecular and Biomolecular Spectroscopy

journal homepage: www.elsevier.com/locate/saa

Characterization and electrochemical studies of Mn(II), Co(II), Ni(II) and Cu(II) complexes with 2-mercapto-3-substituted-quinazolin-4-one and 1,10-phenanthroline or ethylenediamine as ligands

V.A. Sawant, S.N. Gotpagar, B.A. Yamgar, S.K. Sawant, R.D. Kankariya, S.S. Chavan*

Department of Chemistry, Shivaji University, 416 004 Kolhapur (MS), India

ARTICLE INFO

Article history:
Received 24 July 2008
Received in revised form 6 November 2008
Accepted 10 November 2008

Keywords:
Mixed ligands
Quinazoline derivatives
Ethylenediamine
1,10-Phenanthroline
ESR spectra
Cyclic voltammetry

ABSTRACT

Some mixed ligand complexes of the type [M(L^1 or L^2)(**phen** or **en**)(H_2O)Cl], where M = Mn(II), Co(II), Ni(II) and Cu(II); HL^1 = 2-mercapto-quinazolin-4-one; HL^2 = 2-mercapto-3-phenyl-quinazolin-4-one; **phen** = 1,10-phenanthroline; **en** = ethylenediamine have been prepared. All complexes were characterized on the basis of elemental analysis, molar conductance, magnetic susceptibility measurements, IR, UV–vis, ESR and powder X-ray diffraction studies. IR spectra of these complexes reveal that the complex formation occurred through both nitrogen and sulphur atoms. On the basis of electronic spectral data and magnetic susceptibility measurement octahedral geometry has been proposed for the complexes. The ESR spectral data of the Cu(II) complexes showed that the metal–ligand bonds have considerable covalent character. X-ray diffraction studies of Cu(II) complexes are used to elucidate the crystal structure. The electrochemical behaviour of mixed ligand Ni(II) complexes was studied which showed that complexes of **phen** appear at more positive potential as compared to those for corresponding **en** complexes.

1. Introduction

Quinazolines are a class of fused heterocycles that contain the pyrimidine nucleus in their structure. The presence of pyrimidine nucleus in these compounds often leads to very interesting biological and pharmaceutical activities especially anti-inflammatory, anticonvulsant, diuretic, antihypertensive, hypnotic, antimalarial, etc. [1–6]. Recently the quinazolines have been found to possess potent phosphodiesterase inhibitory activity, which is potentially useful in the treatment of asthma [7]. Quinazolines especially containing nitrogen and sulphur donor atoms play an important role in anti-cancer and anti-viral activities. In addition, they can form different types of coordination compounds due to the several electron-rich donor centers with unusual structural and chemical properties [8,9]. Because of the biological importance of quinazoline derivatives and its ability to act as polyfunctional ligand, many studies on its metal complexes have been carried out [10–13]. Ethylenediamine and 1,10-phenanthroline chelators also act as potential antitumor agents and they can show better antitumor activity if they form water-soluble neutral complexes with transition metal ions [14,15]. In this paper we report the mode of bonding of 2-mercapto-quinazolin-4-one (HL^1), 2-mercapto-3-phenyl-quinazolin-4-one (HL^2) as primary ligand and 1,10-phenanthroline (**phen**), ethylenediamine (**en**) as secondary ligand with Mn(II), Co(II), Ni(II) and Cu(II). The complexes prepared were characterized particularly by elemental analysis, conductance, magnetic moment, X-ray crystallography and spectral studies (IR, UV–vis and ESR). Electrochemical behaviour of these complexes has also been discussed.

2. Experimental

2.1. Materials and methods

All chemicals used were of the analytical reagents grade (AR) and of highest purity available. Elemental analysis (C, H, N and S) was performed on a Thermo Finnegan FLASH EA-112 CHNS analyzer. Electronic spectra were recorded on a Shimadzu UV-visible NIR spectrophotometer. Magnetic susceptibility was measured on Gouy balance at room temperature using $Hg[Co(SCN)_4]$ as calibrant. Infrared spectra were recorded on Perkin Elmer FT-IR spectrometer as KBr pellets in the 4000–400 cm^{-1} spectral range. ESR spectra of the complexes were recorded at room temperature on Varian E-112 spectrometer using TCNE as the standard. X-ray powder analysis was carried out by using Philips PW 3710 diffractometer operated at 40 kV and 30 mA generator using Cu Kα line at 1.54056 Å

---

* Corresponding author. Tel.: +91 231 2609164; fax: +91 231 2691533.
E-mail address: sanjaycha2@rediffmail.com (S.S. Chavan).

1386-1425/$ – see front matter © 2008 Elsevier B.V. All rights reserved.
doi:10.1016/j.saa.2008.11.004

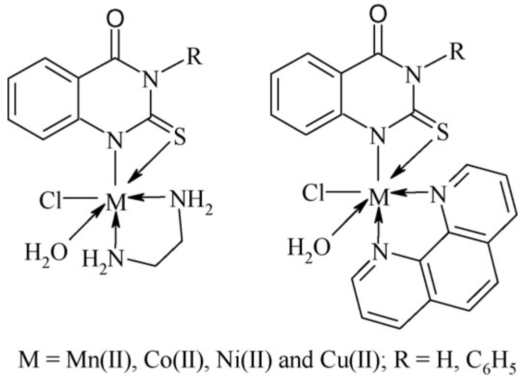

Fig. 1. Proposed molecular structure of mixed ligand complexes.

as the radiation source. Cyclic voltammetry measurements were performed with a CH-400A Electrochemical Analyzer. A standard three-electrode system, consisting of Pt disk working electrode, Pt wire counter electrode and Ag/AgCl reference electrode containing aqueous 3 M KCl were used. All potentials were converted to SCE scale. Tetrabutyl ammonium perchlorate (TBAP) was used as supporting electrolyte and all measurements were carried out in DMF solution at room temperature with scan rate 50 mV s^{-1}.

2.2. Synthesis of HL^1 and HL^2 ligands

2-Mercapto-quinazolin-4-one (HL^1) and 2-mercapto-3-phenyl-quinazolin-4-one (HL^2) were prepared by reported procedure [16,17]. This was characterized by elemental analysis, infrared, ^1H NMR and mass spectra. Satisfactory results were obtained.

2.3. Preparation of mixed ligand complexes (Fig. 1)

The mixed ligand complexes of the ligands (HL^1, HL^2, **phen**, and **en**) were prepared by the addition of hot ethanolic solution (60 °C) of the appropriate metal chloride (1 mmol, 0.197 g, $MnCl_2{\cdot}4H_2O$, 0.237 g, $CoCl_2{\cdot}6H_2O$, 0.237 g, $NiCl_2{\cdot}6H_2O$ and 0.170 g, $CuCl_2{\cdot}2H_2O$) to the hot ethanolic solution of the ligands (1 mmol, 0.178 g, HL^1 or 0.256 g, HL^2 and 0.180 g, **phen** or 0.069 ml, **en**) while stirring. The resultant mixtures were stirred for 2 h where upon the complexes were precipitated. They were collected by filtration, washed with 1:1 ethanol:water mixture, and dried under vacuum over $CaCl_2$ (Fig. 1).

3. Results and discussion

The results of the elemental analysis of the mixed ligand complexes, which are recorded in Table 1, are in good agreement with those required by the proposed formula. The general reaction for the preparation of the mixed ligand complexes of HL^1 or HL^2 (primary ligand) and **phen**, or **en** (secondary ligand) is

$$MCl_2{\cdot}nH_2O + HL^1 \text{ or } HL^2 + \mathbf{phen} \text{ or } \mathbf{en}$$
$$\rightarrow [M(L^1 \text{ or } L^2)(\mathbf{phen} \text{ or } \mathbf{en})(H_2O)Cl]$$

M = Mn(II), Co(II), Ni(II) and Cu(II) and n = 2–6; HL^1 = 2-mercapto-quinazolin-4-one, HL^2 = 2-mercapto-3-phenyl-quinazolin-4-one; **phen** = 1,10-phenanthroline, **en** = ethylenediamine.

3.1. IR spectral studies

The main stretching frequencies of the IR spectra of the ligands and their mixed ligand complexes are presented in Table 2. The ligands HL^1 and HL^2 are capable of exhibiting thione-thiol tau-

Table 1
Analytical and physico-chemical data of the metal complexes.

Complex	M.F. (colour)	Yield	M.P. (°C)	Analytical data % found (calculated)					Λ_M (Ω^{-1} cm^2 mol^{-1})
				M	C	H	N	S	
[Mn(L^1)(**phen**)(H_2O)Cl]	$C_{20}H_{15}N_4O_2SClMn$ (brown)	74	>300	11.64 (11.79)	51.76 (51.57)	3.32 (3.25)	11.81 (12.03)	6.69 (6.88)	21.65
[Co(L^1)(**phen**)(H_2O)Cl]	$C_{20}H_{15}N_4O_2SClCo$ (yellow)	65	>300	12.75 (12.54)	51.46 (51.13)	3.03 (3.22)	12.21 (11.93)	6.68 (6.82)	26.23
[Ni(L^1)(**phen**)(H_2O)Cl]	$C_{20}H_{15}N_4O_2SClNi$ (pale green)	74	>300	12.60 (12.50)	51.22 (51.16)	3.43 (3.22)	11.69 (11.93)	7.05 (6.82)	29.98
[Cu(L^1)(**phen**)(H_2O)Cl]	$C_{20}H_{15}N_4O_2SClCu$ (green)	76	>300	13.53 (13.39)	50.47 (50.63)	3.37 (3.19)	11.62 (11.81)	6.92 (6.74)	20.40
[Mn(L^1)(**en**)(H_2O)Cl]	$C_{10}H_{15}N_4O_2SClMn$ (brown)	72	>300	16.05 (15.89)	34.99 (34.74)	3.99 (4.37)	16.54 (16.20)	9.58 (9.27)	18.32
[Co(L^1)(**en**)(H_2O)Cl]	$C_{10}H_{15}N_4O_2SClCo$ (green)	65	>300	16.66 (16.85)	34.56 (34.34)	4.51 (4.32)	16.28 (16.02)	9.28 (9.16)	19.99
[Ni(L^1)(**en**)(H_2O)Cl]	$C_{10}H_{15}N_4O_2SClNi$ (pale green)	66	>300	16.88 (16.79)	34.67 (34.36)	4.53 (4.32)	16.38 (16.03)	9.32 (9.17)	21.65
[Cu(L^1)(**en**)(H_2O)Cl]	$C_{10}H_{15}N_4O_2SClCu$ (blue)	73	>300	17.61 (17.93)	34.02 (33.89)	4.64 (4.26)	16.04 (15.81)	9.48 (9.15)	12.90
[Mn(L^2)(**phen**)(H_2O)Cl]	$C_{26}H_{19}N_4O_2SClMn$ (brown)	72	>300	10.24 (10.14)	57.88 (57.63)	3.87 (3.53)	10.78 (10.34)	6.05 (5.91)	36.33
[Co(L^2)(**phen**)(H_2O)Cl]	$C_{26}H_{19}N_4O_2SClCo$ (pale yellow)	68	>300	11.08 (10.80)	57.63 (57.20)	3.76 (3.51)	10.06 (10.26)	5.74 (5.87)	29.60
[Ni(L^2)(**phen**)(H_2O)Cl]	$C_{26}H_{19}N_4O_2SClNi$ (pale green)	76	>300	10.88 (10.76)	57.38 (57.23)	3.60 (3.51)	10.19 (10.27)	5.78 (5.88)	15.47
[Cu(L^2)(**phen**)(H_2O)Cl]	$C_{26}H_{19}N_4O_2SClCu$ (green)	72	>300	11.39 (11.54)	56.49 (56.72)	3.63 (3.48)	10.38 (10.18)	5.67 (5.82)	44.41
[Mn(L^2)(**en**)(H_2O)Cl]	$C_{16}H_{19}N_4O_2SClMn$ (brown)	76	>300	13.18 (13.02)	45.32 (45.56)	4.46 (4.54)	13.42 (13.28)	7.41 (7.60)	28.93
[Co(L^2)(**en**)(H_2O)Cl]	$C_{16}H_{19}N_4O_2SClCo$ (green)	69	>300	13.91 (13.84)	45.46 (45.13)	4.78 (4.49)	13.33 (13.15)	7.92 (7.53)	14.13
[Ni(L^2)(**en**)(H_2O)Cl]	$C_{16}H_{19}N_4O_2SClNi$ (pale green)	68	>300	13.45 (13.79)	45.58 (45.15)	4.63 (4.50)	13.46 (13.16)	7.74 (7.53)	18.84
[Cu(L^2)(**en**)(H_2O)Cl]	$C_{16}H_{19}N_4O_2SClCu$ (green)	70	>300	14.42 (14.76)	44.98 (44.64)	4.83 (4.45)	13.32 (13.01)	7.20 (7.44)	42.39

Table 2
Infrared spectral data of the ligands and metal complexes.

Compound	$\nu(H_2O)$	$\nu(NH)_2$	ν(NH)	ν(C=O)	Thioamide bands				ν(M–N)
					I	II	III	IV	
HL^1			3081	1686	1568	1307	978	870	
$[Mn(L^1)$(**phen**)$(H_2O)Cl]$	3445		3060	1690	1567, 1505	1299	978	857	461
$[Co(L^1)$(**phen**)$(H_2O)Cl]$	3460		3065	1689	1568, 1507	1300	978	865	459
$[Ni(L^1)$(**phen**)$(H_2O)Cl]$	3478		3060	1697	1560, 1507	1295	980	860	465
$[Cu(L^1)$(**phen**)$(H_2O)Cl]$	3432		3056	1700	1549, 1505	1327	976	863	455
$[Mn(L^1)$(**en**)$(H_2O)Cl]$	3436	3235, 3300	3063	1690	1554, 1504	1323	977	857	469
$[Co(L^1)$(**en**)$(H_2O)Cl]$	3440	3230, 3298	3056	1700	1540, 1505	1319	979	860	459
$[Ni(L^1)$(**en**)$(H_2O)Cl]$	3478	3240, 3296	3059	1690	1558, 1504	1329	977	857	461
$[Cu(L^1)$(**en**)$(H_2O)Cl]$	3421	3232, 3300	3060	1697	1560, 1507	1295	980	863	460
HL^2			3245	1680	1533	1339	988	842	
$[Mn(L^2)$(**phen**)$(H_2O)Cl]$	3442			1686	1566, 1540	1316	989	835	465
$[Co(L^2)$(**phen**)$(H_2O)Cl]$	3435			1682	1560, 1538	1298	988	837	454
$[Ni(L^2)$(**phen**)$(H_2O)Cl]$	3447			1698	1579, 1540	1320	991	832	460
$[Cu(L^2)$(**phen**)$(H_2O)Cl]$	3436			1686	1566, 1541	1303	985	836	463
$[Mn(L^2)$(**en**)$(H_2O)Cl]$	3460	3232, 3300		1698	1573, 1540	1320	986	835	465
$[Co(L^2)$(**en**)$(H_2O)Cl]$	3430	3237, 3296		1702	1566, 1543	1316	990	837	458
$[Ni(L^2)$(**en**)$(H_2O)Cl]$	3420	3240, 3300		1695	1570, 1541	1320	991	832	470
$[Cu(L^2)$(**en**)$(H_2O)Cl]$	3433	3232, 3299		1700	1573, 1543	1305	977	837	459

Thioamide bands: band-I (δNH + δC–N); band-II (νC=N + δNH + δCH + νC=S); band-III (νC=S + νC=N); band-IV (νC=S).

tomerism. In the IR spectra of HL^1 and HL^2, ν(NH) band appeared at 3081 and 3248 cm^{-1} respectively and absence of ν(SH) band near 2600 cm^{-1} indicates the thione structural form of the ligands in solid state. The shifting of ν(NH) band to lower frequency (3065–3056 cm^{-1}) in the complexes of HL^1 and disappeared in the complexes of HL^2, providing a strong evidence for involvement of ligand coordination in deprotonated form. This is also supported by the appearance of ν(M–N) band at 470–459 cm^{-1} in the complexes. The characteristic ν(C=O) frequency of ligands HL^1 and HL^2 occurs at 1686 and 1680 cm^{-1} remains unaltered in all complexes, indicates absence of bonding through carbonyl oxygen of HL^1 and HL^2 [18].

Both the HL^1 and HL^2 contain a thioamide group (H–N–C=S) and give rise to four characteristic bands (I–IV) at 1568, 1307, 978, 870 and 1533, 1339, 988, 842 cm^{-1} in their infrared spectra respectively [18]. The thioamide band-I [δ(NH) + δ(C–N)] observed at 1568 and 1533 cm^{-1} respectively in HL^1 and HL^2, splits up in the spectra of the complexes also suggests the coordination through imino nitrogen atom of HL^1 and HL^2. The two bands appearing at the frequency 1307, 1339 cm^{-1} [ν(C=N) + δ(NH) + δ(CH) + ν(C=S)] thioamide band-II and 870, 842 cm^{-1} [ν(C=S)] thioamide band-IV respectively in the spectra of HL^1 and HL^2 have been shifted to lower frequencies in the ranges 1329–1295 cm^{-1} and 865–832 cm^{-1} indicating coordination of thione/thiolato sulphur. The thioamide band-III observed at 978 and 988 cm^{-1} in HL^1 and HL^2 reduced in intensity on coordination with metal ion [19]. In the spectra of mixed **phen** complexes the bands of **phen**-free ligand at 740 cm^{-1} are shifted to higher frequencies around 777 cm^{-1} in the complexes. The spectra of mixed **en** complexes show two characteristic bands at 3232 and 3300 cm^{-1} assigned to ν_{sym} and ν_{asym} vibration of NH_2 suggesting coordination through NH_2 [20]. The presence of a broad weak band around 3440 cm^{-1} in the spectra of all complexes is associated with coordinated water molecules [21].

3.2. *Molar conductivity*

The solubility of the complexes in DMF permitted calculation of the molar conductivity of 10^{-3} M solutions at 25 °C and, by comparison, the electrolytic nature of each complex (Table 1). The complexes are found to be non-electrolytic in DMF solution, implying the coordination of halide anion. Elemental analysis identified the complexes as $[M(L^1$ or $L^2)$(**phen** or **en**)$(H_2O)Cl]$.

3.3. *Magnetic moments and electronic spectra*

Magnetic moments and electronic spectra of the metal complexes are listed in Table 3. In all metal complexes, the absorption bands at 45,454, 40,816, 35,842, 34,013, 31,347 and 44,444, 40,816,

Table 3
Electronic spectral data and magnetic moment values of the metal complexes.

Compound	μ_{eff} (μ_B)	$\pi \to \pi^*$ and $n \to \pi^*$ transitions and charge transfer transitions (cm^{-1})	$d \to d$ transitions (cm^{-1})
HL^1		45,454, 40,816, 35,842, 34,013, 31,347	–
$[Mn(L^1)$(**phen**)$(H_2O)Cl]$	5.86	37,453, 34,602, 28,571	19,801, 16,000, 14,005
$[Co(L^1)$(**phen**)$(H_2O)Cl]$	4.85	38,167, 34,364, 28,735	20,876, 15,267
$[Ni(L^1)$(**phen**)$(H_2O)Cl]$	2.76	38,022, 34,482, 29,673	15,380
$[Cu(L^1)$(**phen**)$(H_2O)Cl]$	1.84	37,735, 34,965, 28,571	15,748
$[Mn(L^1)$(**en**)$(H_2O)Cl]$	5.90	38,461, 34,602, 29,673	20,000, 16,129, 13,888
$[Co(L^1)$(**en**)$(H_2O)Cl]$	4.88	37,735, 34,482, 29,850	21,276, 15,386
$[Ni(L^1)$(**en**)$(H_2O)Cl]$	2.88	38,022, 34,843, 29,411	16,025
$[Cu(L^1)$(**en**)$(H_2O)Cl]$	1.79	37,037, 34,482, 29,239	15,873
HL^2		44,444, 40,816, 36,363, 34,013, 28,818	–
$[Mn(L^2)$(**phen**)$(H_2O)Cl]$	5.89	38,022, 34,965, 27,777	19,531, 16,025, 13,947
$[Co(L^2)$(**phen**)$(H_2O)Cl]$	4.73	36,496, 33,783, 27,247	20,876, 14,727
$[Ni(L^2)$(**phen**)$(H_2O)Cl]$	2.82	36,764, 33,898, 27,472	16,000
$[Cu(L^2)$(**phen**)$(H_2O)Cl]$	1.89	37,397, 34,843, 27,624	15,384
$[Mn(L^2)$(**en**)$(H_2O)Cl]$	5.92	37,453, 34,482, 27,027	19,607, 16,660, 13,908
$[Co(L^2)$(**en**)$(H_2O)Cl]$	4.74	37,037, 34,482, 27,397	21,505, 14,925
$[Ni(L^2)$(**en**)$(H_2O)Cl]$	2.98	36,496, 33,898, 27,247	15,830
$[Cu(L^2)$(**en**)$(H_2O)Cl]$	1.80	39,215, 34,482, 27,472	14,738

Table 4
Spin Hamiltonian parameters of polycrystalline Cu(II) complexes.

Complex	$g_{\|\|}$	$g_{\perp}$	g_{avg}	$A_{\|\|}(\times10^{-4}\,cm^{-1})$	$A_{\perp}(\times10^{-4}\,cm^{-1})$	α^2	β^2	G
[Cu(L^1)(**phen**)(H$_2$O)Cl]	2.271	2.073	2.139	168	65	0.737	0.873	3.71
[Cu(L^1)(**en**)(H$_2$O)Cl]	2.155	2.053	2.087	196	56	0.593	0.619	2.92
[Cu(L^2)(**phen**)(H$_2$O)Cl]	2.224	2.060	2.114	168	58	0.707	0.728	3.73
[Cu(L^2)(**en**)(H$_2$O)Cl]	2.155	2.066	2.095	196	47	0.599	0.569	2.35

36,363, 34,013, 28,818 cm^{-1} due to $\pi\rightarrow\pi^*$ and $n\rightarrow\pi^*$ transitions that are observed in the spectra of the free ligands HL^1 and HL^2 shifted to blue or red frequencies due to the coordination of the ligand with metal ions.

The Mn(II) complexes exhibit three weak absorption bands at 14,005–13,888, 16,660–16,000 and 20,000–19,531 cm^{-1} attributed to $^6A_{1g}\rightarrow{}^4T_{1g}(\nu_1)$, $^6A_{1g}\rightarrow{}^4T_{2g}(\nu_2)$ and $^6A_{1g}\rightarrow{}^4E_g$, $^4A_{1g}(\nu_3)$ transitions respectively. These absorptions are consistent with an octahedral geometry around Mn(II) in all complexes. The magnetic moment values of Mn(II) complexes in the range 5.86–5.92μ_B are an indicative of octahedral geometry [22].

The electronic spectra of Co(II) complexes display two bands in the range of 15,386–14,727 and 21,505–20,876 cm^{-1} may be assigned to $^4T_{1g}(^4F)\rightarrow{}^4A_{2g}(^4F)$ and $^4T_{1g}(^4F)\rightarrow{}^4T_{1g}(^4P)$ indicating octahedral configuration around Co(II) ion. Three spin allowed transition for octahedral Co(II) complexes is expected: $^4T_{1g}(^4F)\rightarrow{}^4T_{2g}(^4F)(\nu_1)$, $^4T_{1g}(^4F)\rightarrow{}^4A_{2g}(^4F)(\nu_2)$, $^4T_{1g}(^4F)\rightarrow{}^4T_{1g}(^4P)(\nu_3)$. The first band appeared in the region 8080–8050 cm^{-1} usually in the IR region, so ν_1 transition due to transition $^4T_{1g}(^4F)\rightarrow{}^4T_{2g}(^4F)$ could not be observed in all the complexes [23]. The μ_{eff} value measured for the Co(II) complexes are in the range 4.73–4.88μ_B respectively which is fairly close to those reported for the unpaired electrons of Co(II) ion in an octahedral environment [24].

In the electronic spectrum of Ni(II) complexes a broad absorption band at 16,025–15,380 cm^{-1} which may be assigned to $^3A_{1g}(F)\rightarrow{}^3T_{2g}(F)$, while the absorption band due to $^3A_{2g}(F)\rightarrow{}^3T_{1g}(P)$, is overlapped with the ligand absorption bands. This indicates that the Ni(II) has an octahedral geometry. The room temperature magnetic moment values of Ni(II) complexes are 2.76–2.98μ_B, which are in normal range observed for octahedral Ni(II) complexes [25].

The electronic spectra of Cu(II) mixed complexes show a broad, low intensity shoulder band centered at 15,873–14,738 cm^{-1} that forms part of the charge transfer band. The ^2E_g and $^2T_{2g}$ states of the octahedral Cu(II) (d^9) split under the influence of tetrahedral distortion and distortion can be such as to cause three transition $^2B_{1g}\rightarrow{}^2B_{2g}$, $^2B_{1g}\rightarrow{}^2E_g$ and $^2B_{1g}\rightarrow{}^2A_{1g}$ to remain unresolved in the spectra [26]. It is concluded that, all three transitions lie within the single broad envelope centered at the same range. This assignment is in agreement with the general observation that Cu(II) d–d transitions are normally close in energy. The octahedral geometry of Cu(II) ion in all complexes is confirmed by the measured magnetic moment values in the range 1.79–1.89μ_B which is in harmony with the reported value [27].

3.4. ESR spectral study

To obtain further information about the stereochemistry and the site of the metal ligand bonding and to determine the magnetic interaction in the metal complexes, the X-band ESR spectra of all copper(II) complexes have been recorded in the polycrystalline state. The spin Hamilton parameters of the complexes were calculated and are summarized in Table 4.

The room temperature polycrystalline ESR spectra of all Cu(II) complexes (Fig. 2) are quite similar and exhibit an auxiliary symmetric g-tensor parameters with $g_{||} > g_{\perp} > 2.0023$ indicating that the copper site has a $d_{x^2-y^2}$ ground state characteristic of octahedral geometry [28]. According to Hathaway [29,30], if the value of G is greater than four, the exchange interaction between copper(II) centers in the solid state is negligible, whereas when is less than four, a considerable exchange interaction is indicated in the solid complex. The calculated G values are given in Table 4. The G values within the range 2.35–3.73 for all copper complexes are consistent with $d_{x^2-y^2}$ ground state.

Apart from this, the covalency parameters α^2 (covalent in-plane σ-bonding) and β^2 (covalent in-plane π-bonding) were calculated

Table 5
X-ray diffraction data of [Cu(L^1)(**en**)(H$_2$O)Cl].

d (Å)	I/I_0	Observed $\sin^2\theta$	Calculated $\sin^2\theta$	$h\,k\,l$	Observed 2θ	Calculated 2θ
13.820	28.2	31.1	31.1	0 1 0	6.39	6.39
8.238	100	87.4	87.4	1 0 0	10.73	10.73
6.830	7.2	127.2	127.2	1 1 0	12.95	12.95
5.095	8.4	228.5	228.5	0 1 1	17.39	17.39
4.856	5.8	251.5	251.5	−1,0,1	18.25	18.25
4.605	5.2	279.7	279.7	−1,1,1	19.25	19.25
4.390	24.1	307.8	306.7	1 0 1	20.21	20.17
4.124	7.9	348.7	349.7	2 0 0	21.52	21.56
3.620	6.5	452.5	453.8	0,−3,1	24.57	24.60
3.500	21.6	484.3	486.2	−2,0,−1	25.42	25.48
3.427	10.3	505.1	505.7	−2,1,1	25.98	25.99
3.211	5.0	575.3	577.2	−2,3,0	27.75	27.80
3.026	11.8	647.8	650.8	2 1 1	29.49	29.56
2.877	18.0	716.6	711.9	0 4 1	31.06	30.95
2.717	11.2	803.3	800.4	−2,−3,1	32.93	32.87
2.488	14.4	957.7	960.6	1 1 2	36.06	36.11
2.443	6.5	993.7	992.8	1,−2,2	36.75	36.73
2.200	5.0	1225.3	1226.6	2 0 2	40.98	41.00
1.930	5.4	1591.6	1592.5	4 2 0	47.03	47.04

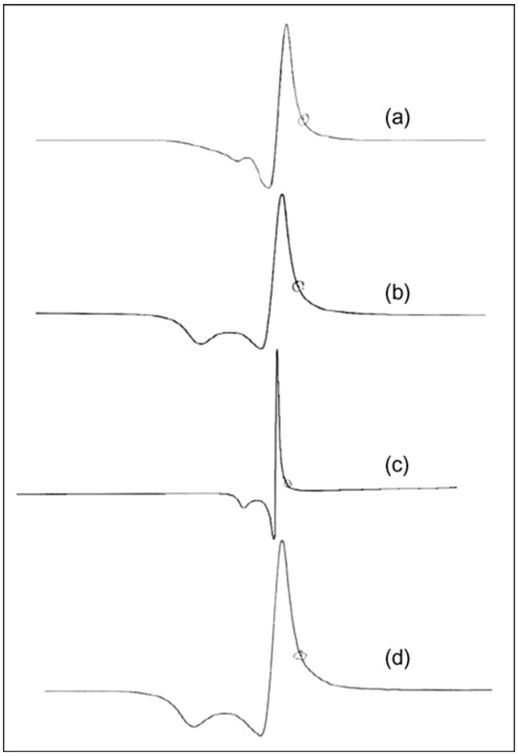

Fig. 2. X-band polycrystalline ESR spectra of the complexes [Cu(L^1)(**Phen**)(H_2O)Cl] (a), [Cu(L^1)(**en**)(H_2O)Cl] (b), [Cu(L^2)(**phen**)(H_2O)Cl] (c), and [Cu(L^2)(**en**)(H_2O)Cl] (d).

using the following equations [31–33]. Where $\alpha^2 = 1.0$ indicates complete ionic character whereas $\alpha^2 = 0.5$ denoted 100% covalent bonding, with assumption of negligible small values of the overlap integral.

$$\alpha^2 = -\frac{A_{||}}{0.036} + \frac{g_{||}}{2.0023} + \frac{3}{7}(g_\perp - 2.0023) + 0.04$$

$$\beta^2 = \frac{(g_{||} - 2.0023)E}{-8\lambda\,\alpha^2}$$

where $\lambda = -828\,\text{cm}^{-1}$ for free copper ion and E is electronic transition energy. From Table 4, the α^2 and β^2 values indicate that there is a substantial interaction in the in-plane σ-bonding whereas the in-plane π-bonding is almost ionic. The lower value of α^2 compared to β^2 indicates that the in-plane σ-bonding is more covalent than in-plane π-bonding. These data are well in accordance with other reported values [34]. Based on these observations, a distorted octahedral geometry is proposed for the complexes. The ESR study of the copper(II) complexes has provided supportive evidence to the conclusion obtained on the basis of electronic spectrum and magnetic moment value.

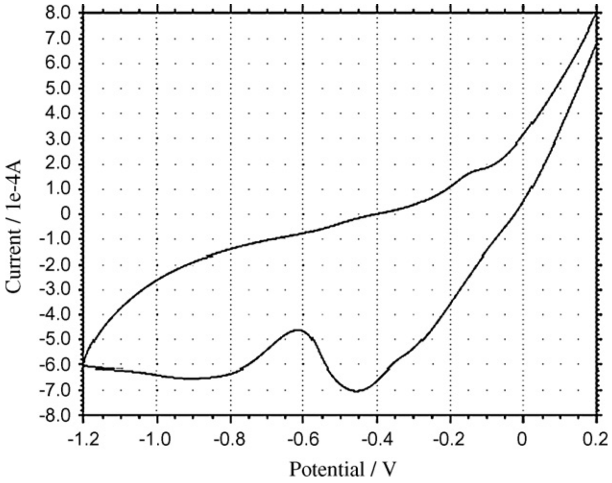

Fig. 3. Cyclic voltammogram of HL^1.

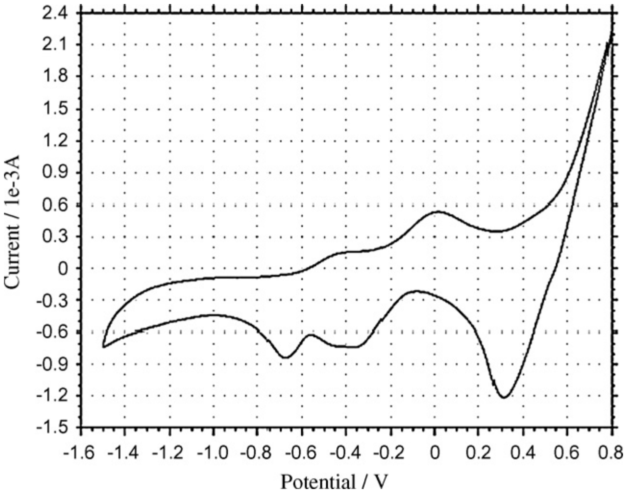

Fig. 4. Cyclic voltammogram of [Ni(L^1)(**en**)(H_2O)Cl].

Table 6
X-ray diffraction data of [Cu(L^2)(**en**)(H_2O)Cl].

d (Å)	I/I_0	Observed $\sin^2\theta$	Calculated $\sin^2\theta$	$h\,k\,l$	Observed 2θ	Calculated 2θ
8.139	100	89.5	89.5	0 1 0	10.86	10.86
5.041	3.3	233.4	233.4	−1,1,0	17.58	17.58
4.846	3.6	252.6	252.6	1 1 0	18.29	18.29
4.595	5.1	281.0	281.0	0 1 1	19.30	19.30
4.363	2.7	311.6	311.6	−1,−1,1	20.33	20.33
4.106	3.6	351.8	351.8	−1,1,1	21.62	21.62
3.596	2.0	458.7	460.6	0,−2,1	24.74	24.79
3.476	12.3	491.0	492.4	−1,2,0	25.60	25.64
3.401	6.1	512.7	517.1	1 1 1	26.17	26.29
3.014	6.9	653.0	654.4	−1,0,2	29.61	29.64
2.865	4.6	722.7	722.5	2 1 0	31.19	31.19
2.472	14.4	970.9	968.6	−2,0,2	36.31	36.27
1.993	2.1	1493.6	1499.4	3 1 0	45.47	45.56
1.924	4.5	1602.8	1609.6	−1,3,2	47.20	47.31
1.631	1.9	2229.4	2227.7	−2,−3,3	56.35	56.33

Table 7
Electrochemical data for ligands and nickel complexes.

Compound	Reduction potentials (*V*)				Oxidation potentials (*V*)			
	E_{pa}	E_{pc}	ΔE_p	$E_{1/2}$	E_{pa}	E_{pc}	ΔE_p	$E_{1/2}$
HL^1	−0.90, −0.45							
[Ni(L^1)(**phen**)(H_2O)Cl]	−0.72	−0.95	0.23	−0.83	0.35	0.20	0.15	0.27
[Ni(L^1)(**en**)(H_2O)Cl]	−0.68	−0.91	0.23	−0.79	0.27	0.04	0.23	0.15
HL^2	−0.66, −0.28							
[Ni(L^2)(**phen**)(H_2O)Cl]	−1.05	−1.15	0.10	−1.10	0.67	0.55	0.12	0.61
[Ni(L^2)(**en**)(H_2O)Cl]	−0.67	−0.36	0.31	−0.52	0.33	0.05	0.28	0.19

Supporting electrolyte: *n*-Bu_4NClO_4 (0.05 M); complex: 0.001 M; solvent: DMF; $\Delta E_p = E_{pa} - E_{pc}$ where, E_{pa} and E_{pc} are anodic and cathodic potentials, respectively; $E_{1/2} = 1/2(E_{pa} + E_{pc})$; scan rate: 50 mV s^{-1}.

3.5. X-ray powder diffraction

Single crystal X-ray crystallographic investigation is the most precise source of information regarding the structure of the complexes, the difficulty of obtaining crystalline complexes in proper symmetric form has rendered the powder X-ray diffraction method for such study. The X-ray diffraction pattern of the complexes [Cu(L^1)(**en**)(H_2O)Cl] and [Cu(L^2)(**en**)(H_2O)Cl] indicates high crystallinity of the complexes. The diffractogram of [Cu(L^1)(**en**)(H_2O)Cl] complex records 19 reflections between 5° and 80° (2θ) with maximum at $2\theta = 10.730°$ corresponding to value of $d = 8.238$ Å (Table 5). The diffractogram of [Cu(L^2)(**en**)(H_2O)Cl] complex consists of 15 reflections with maxima at $2\theta = 10.860°$ corresponding to value of $d = 8.139$ Å (Table 6). The main peaks of [Cu(L^1)(**en**)(H_2O)Cl] and [Cu(L^2)(**en**)(H_2O)Cl] complexes have been indexed by using computer software by trial and error method [35,36], keeping in mind characteristics of various symmetry systems till good fit could be obtain between observed and calculated 2θ and $\sin^2\theta$ values. The method also yielded *h k l* (miller indices) values. The relative intensities corresponding to the prominent peaks have been measured.

The indexing of diffractogram of [Cu(L^1)(**en**)(H_2O)Cl] and [Cu(L^2)(**en**)(H_2O)Cl] complexes is identical. Based on this it can be proposed that these compounds belong to same structural class. A comparison of values of 2θ and $\sin^2\theta$ for the [Cu(L^1)(**en**)(H_2O)Cl] and [Cu(L^2)(**en**)(H_2O)Cl] complexes reveals that, there is good agreement between the calculated and observed values of 2θ and $\sin^2\theta$ on the basis of assumption of triclinic structure [37]. The small difference in the observed *d* spacing can be attributed to difference in unit cell dimensions. The structure of [Cu(L^1)(**en**)(H_2O)Cl] complex yields values for lattice constant $a = 8.311$ Å, $b = 13.874$ Å, and $c = 5.598$ Å; $\alpha = 91.666°$, $\beta = 95.959°$, and $\gamma = 94.578°$; unit cell volume $V = 639.56$ Å^3. However the structure of [Cu(L^2)(**en**)(H_2O)Cl] complex yields values for lattice constant $a = 6.392$ Å, $b = 8.202$ Å, and $c = 6.268$ Å; $\alpha = 96.723°$, $\beta = 103.226°$, and $\gamma = 90.735°$; unit cell volume $V = 317.55$ Å^3. In conjugation with these lattice parameters the conditions such as $a \neq b \neq c$ and of $\alpha \neq \beta \neq \gamma$ required for the samples to be triclinic were tested and found to be satisfactory.

3.6. Electrochemical studies

Electrochemical properties of the ligands HL^1 and HL^2 and their Ni(II) complexes were investigated in DMF solution containing 0.05 M *n*-Bu_4NClO_4 as supporting electrolyte by cyclic voltammetry (Table 7). All the measurements were carried out in 10^{-3} M solutions at room temperature in the potential range +1 to −1.5 V with scan rate 50 mV s^{-1}. Typical cyclic voltammogram (CV) of HL^1 and its [Ni(L^1)(**en**)(H_2O)Cl] complex are shown in Figs. 3 and 4 respectively.

Ligands HL^1 and HL^2 displayed waves at E_{pa} values −0.90, −0.45 V and −0.66, −0.28 V, respectively corresponding to irreversible oxidation of ligand. The electrochemical potentials of the complexes were characterized by well-defined waves in cathodic and anodic regions. Since the ligands used in this work are not reversibly oxidized or reduced in the applied potential range, the redox processes are assigned to the metal centers only.

All the Ni(II) complexes exhibit both anodic and cathodic redox potentials. In anodic potential region the reduction wave (E_{pc}, 0.04–0.55 V) corresponding to Ni(III)/Ni(II) reaction is obtained. During the reverse scan the oxidation of Ni(II)/Ni(III) occurs in the potential range (E_{pa}, 0.27–0.67 V). In cathodic potential region the reduction wave (E_{pc}, −0.36 to −1.15 V) corresponding to Ni(II)/Ni(I) reaction is obtained. During the reverse scan the oxidation of Ni(I)/Ni(II) occurs in the potential range (E_{pa}, −0.67 to −1.05 V). However the values of the limiting peak-to-peak separation (ΔE_p) ranging from 100 to 310 mV reveal that this process can be quassi-reversible.

Further the redox process among the mixed ligand Ni(II) complexes of **phen** appears at more positive potential (0.27 V) as compared to those for corresponding **en** complex (0.15 V). This trend may be due to the strong σ-donor tendency of the ethylenediamine moiety and the strong π-acceptor ability of 1,10-phenanthroline ligand. These results are consistent with those reported in the literature [38]. In comparison with [Ni(L^1)(**en**)(H_2O)Cl] (0.15 V) the respective response of [Ni(L^2)(**en**)(H_2O)Cl] (0.19 V) are shifted to a more positive potential. This indicates that the coordination of nickel to the ligand lessens its electron-withdrawing properties [39].

4. Conclusion

A series of mixed ligand complexes of 2-mercapto-quinazolin-4-one (HL^1), 2-mercapto-3-phenyl-quinazolin-4-one (HL^2) and 1,10-phenanthroline (**phen**), ethylenediamine (**en**) with Mn(II), Co(II), Ni(II) and Cu(II) have been synthesized and characterized. All complexes exhibit octahedral geometry by involvement of both nitrogen and sulphur of HL^1 and HL^2 ligands in complex formation. All the Ni(II) complexes exhibit both positive and negative redox potentials corresponding to Ni(III)/Ni(II) and Ni(II)/Ni(I) processes respectively. Further, the redox potential of Ni(II) complexes of phenanthroline is higher than Ni(II) complexes of ethylenediamine. The complex crystallizes in the triclinic crystal system.

Acknowledgements

Authors are thankful to IISc, Bangalore for Elemental Analysis and Regional Sophisticated Instrumentation Centre, IIT, Mumbai for providing ESR facility.

References

[1] V. Alagarsamy, V. Muthukumar, N. Pavalarani, P. Vasanthanathan, R. Revathi, Biol. Pharm. Bull. 26 (2003) 557–559.
[2] J.H. Chan, J.S. Hong, L.F. Kuyper, M.L. Jones, D.P. Baccanari, R.L. Tansik, C.M. Boytos, S.K. Rudolph, A.D. Brown, J. Heterocycl. Chem. 34 (1997) 145–151.
[3] R.O. Dempcy, E.B. Skibo, Biochemistry 30 (1991) 8480–8487.
[4] I.R. Prous (Ed.), Drugs Future 18 (1993) 475.

[5] Nordisk-Droge, 18113; N.A. Patent, (ed.); Nordisk-Droge and Kemi-Kalieforretning AIS, Netherlands, 1965.
[6] S. Johne, Pharmazie 36 (1981) 583–596.
[7] A.J. Duplantier, J.B. Cheng, Ann. Rep. Med. Chem. 29 (1994) 73–81.
[8] B. Prabhakar, P. Lingaiah, K. Laxma Reddy, Polyhedron 9 (1990) 805–811.
[9] K.B. Gudasi, S.A. Patil, R.S. Vadavi, R.V. Shenoy, Trans. Met. Chem. 31 (2006) 586–592.
[10] B. Prabhakar, P. Lingaiah, K. Laxma Reddy, Proc. Indian Acad. Sci. (Chem. Sci.) 103 (1991) 599–605.
[11] K.B. Gudasi, R.S. Vadavi, R.V. Shenoy, M.S. Patil, S.A. Patil, M. Nethaji, Trans. Met. Chem. 30 (2005) 661–668.
[12] K.B. Gudasi, V.C. Havanur, S.A. Patil, B.R. Patil, Metal Based Drugs, 2007, Article ID 37348, 7.
[13] K. Siddappa, T. Reddy, M. Mallikarjun, C.V. Reddy, E-J. Chem. 5 (2008) 155–162.
[14] D.R. McMillin, K.M. McNett, Chem. Rev. 99 (1999) 1201–1220.
[15] K.E. Erkkila, D.T. Odom, J.K. Barton, Chem. Rev. 98 (1998) 2777–2796.
[16] P.B. Talukdar, S.K. Sengupta, A.K. Datta, T.K. Roy, Indian J. Chem. B 15 (1977) 41–45.
[17] A.S. El-Azab, Phosphorus Sulfur Silicon 182 (2007) 333–348.
[18] B. Singh, M.M.P. Rukhaiyar, R.J. Sinha, J. Inorg. Nucl. Chem. 39 (1977) 29–32.
[19] P.F. Raphel, E. Manoj, M.R. Prathapachandra Kurup, Polyhedron 26 (2007) 818–828.
[20] C.C. Su, T.Y. Tai, S.P. Wu, S.L. Wang, F.L. Liao, Polyhedron 18 (1999) 2361–2368.
[21] I. Yilmaz, H. Temel, H. Alp, Polyhedron 27 (2008) 125–132.
[22] V.P. Daniel, B. Murukan, B. Sindhu Kumari, K. Mohanan, Spectrochim. Acta Part A 70 (2008) 403–410.
[23] B.K. Singh, P. Mishra, B.S. Garg, Spectrochim. Acta Part A 69 (2008) 880–888.
[24] Z.H. Abd El-Wahab, Spectrochim. Acta Part A 67 (2007) 25–38.
[25] E.K. Efthimiadou, Y. Sanakis, N. Katsaros, A. Karaliota, G. Psomas, Polyhedron 26 (2007) 1148–1158.
[26] J. Kohout, M. Hvastijova, J. Kozisek, J.G. Diaz, M. Valko, L. Jager, I. Svoboda, Inorg. Chim. Acta 287 (1999) 186–192.
[27] N.R.S. Kumar, M. Nethaji, K.C. Patil, Polyhedron 10 (1991) 365–371.
[28] G. Speir, J. Csihony, A.M. Whalen, C.G. Pierpont, Inorg. Chem. 35 (1996) 3519–3524.
[29] B.J. Hathaway, D.E. Billing, Coord. Chem. Rev. 5 (1970) 143–207.
[30] B.J. Hathaway, Struct. Bond. 57 (1984) 55.
[31] R.K. Ray, G.R. Kauffman, Inorg. Chim. Acta 173 (1990) 207–214.
[32] K. Jayasubramanian, S.A. Samath, S. Thambidurai, R. Murugesan, S.K. Ramalingam, Trans. Met. Chem. 20 (1995) 76–80.
[33] V.S.X. Anthonisamy, R. Murugesan, Chem. Phys. Lett. 287 (1998) 353–358.
[34] R.P. John, A. Sreekanth, M.R.P. Kurup, A. Usman, A.R. Ibrahim, H.-K. Fun, Spectrochim. Acta Part A 59 (2003) 1349–1358.
[35] H.P. Klug, L.E. Alexander, X-ray Diffraction Procedure for Polycrystalline and Amorphous Materials, John Wiley, London, NY, 1974.
[36] B.D. Cullity, Elements of X-ray Diffraction, second ed., Addison-Wesley, 1977.
[37] G. Pandey, K.K. Narang, J. Coord. Chem. 59 (2006) 1495–1507.
[38] P.B. Sammani, P.K. Bhattacharya, P.A. Ganeshpure, V.J. Koshy, S. Satish, J. Mol. Catal. A: Chem. 110 (1996) 89–94.
[39] C.D. Papadopoulos, A.G. Hatzidimitriou, G.P. Voutsas, M. Lalia-Kantouri, Polyhedron 26 (2007) 1077–1086.